J. Math. Anal. Appl. 385 (2012) 354–370

Contents lists available at ScienceDirect

Journal of Mathematical Analysis and Applications

www.elsevier.com/locate/jmaa

Quasi-optimized Schwarz methods for reaction diffusion equations with time delay

Shu-Lin Wu [a,*], Cheng-Ming Huang [b]

[a] School of Science, Sichuan University of Science and Engineering, Zigong, Sichuan 643000, PR China
[b] School of Mathematics and Statistics, Huazhong University of Science and Technology, Wuhan 430074, PR China

ARTICLE INFO

Article history:
Received 11 March 2010
Available online 14 July 2011
Submitted by W. Layton

Keywords:
Schwarz waveform relaxation
Reaction diffusion equations
Time delay
Optimization

ABSTRACT

In this paper, we investigate the convergence behavior of the Schwarz waveform relaxation (SWR) algorithms for solving PDEs with time delay. We choose the reaction diffusion equations with a constant time delay as the underlying model problem and try to derive optimized transmission conditions of Robin type. To this end, we propose a new method to get quasi-optimized parameter involved in the transmission conditions and it is shown that this method is essentially different from the existing ones. Moreover, when the situation is reduced into the heat equations with a constant delay, we show that this method results in a more efficient quasi-optimized parameter. Numerical results are provided to validate our theoretical results.

1. Introduction

Delay PDEs arise from various applications, like biology, medicine, control theory, climate models, and many others (see e.g. Wu [23] and the references therein). A delay PDE differs from a regular PDE in that it depends not only on the solution at a present stage but also on the solution at some past stage(s). If, additionally, the equation depends on the derivative(s) of the solution at some past stage(s), then it is a neutral delay PDE. Delay PDEs are also called partial functional differential equations as their unknown solutions are used in these equations as functional arguments.

While the theoretical properties of delay PDEs have been investigated deeply and widely in the past years, there is little experience with numerical methods for solving delay PDEs, particularly with parallel computational methods. Zubik-Kowal and Vandewalle [25] analyzed the convergence of the waveform relaxation methods [15,21] of Gauss–Seidel and Jacobi type, for solving the discretized delay PDE problems. In that paper, they presented a first analysis of domain decomposition based waveform relaxation methods for the solution of two model delay PDEs.

Waveform relaxation schemes using domain decomposition in space for PDEs are terminologically called *Schwarz waveform relaxation* (SWR) algorithms. The algorithms are characterized by firstly partitioning the spatial domain into overlapping subdomains, and then solving simultaneously inside each subdomain through iterations. We refer to [7,11,12,10] for the original idea of this kind of domain decomposition algorithms.

Due to the excellent capability in parallel computation of PDEs, the SWR algorithms are becoming more and more popular, particularly in the field of solving time dependent problems. It is a common point that the SWR algorithms can be classified into two categories depending on the used transmission conditions between subdomains: the classical SWR algorithms and the optimized ones. For the classical SWR algorithms, Dirichlet conditions are used as transmission conditions (see, e.g., [2–4,6,7,9–13,18]), and in such case the overlap between adjacent subdomains is essentially important to

* Corresponding author.
E-mail addresses: wushulin_ylp@163.com (S.-L. Wu), chengming_huang@hotmail.com (C.-M. Huang).

0022-247X/$ – see front matter
doi:10.1016/j.jmaa.2011.06.052

guarantee the convergence. It has been shown in [14] that, the Dirichlet condition inhibits the information exchange between subdomains and therefore the convergence speed of the classical SWR algorithms is slowed down. To speed up the convergence rate of the SWR algorithms, new transmission conditions are introduced in [14] and [1]. The new transmission conditions always involve one or two free parameters which can be used to optimize the convergence rate of the SWR algorithm. Hence, the new algorithm is usually called *optimized* SWR algorithms. For regular linear PDEs, the optimization problem arising in determining the best parameters involved in the transmission conditions can be solved in closed formulas. The interested reader can refer to the work by Gander and Halpern [14] for Robin type transmission conditions and to the work by Bennequin et al. [1] for higher order conditions.

Nowadays, optimized SWR algorithms become more and more popular in scientific and engineering computing due to the much faster convergence speed compared to the classical SWR algorithms, and have been adopted to solve more complex problems arising from physics and engineering. For example, [8] applied the algorithms to the equations of ferro-magnetics in the micro-magnetic model; [20,19] and [5] investigated the applications to the shallow-water problem and Maxwell's equations, respectively.

However, for PDEs with time delay, the situation becomes very complex and concrete results about convergence behavior of both the classical and the optimized SWR algorithms are rare. For example, the superlinear convergence of the classical SWR algorithm can be easily obtained for the regular linear parabolic PDEs by using standard inverse Fourier transform (see, e.g., [4,14,13]), while it is difficult and still unknown when time delay is taken into account. In the seminal paper [22], Vandewalle and Gander have shown that, the techniques that are used to analyze the classical and optimized SWR algorithms cannot be straightforwardly applied to PDEs with time delay. In that paper, two representative model problems are considered: a PDE with a constant delay and one with a distributed delay. For the classical SWR algorithms, by using elementary but very technical arguments, Vandewalle and Gander presented an estimate of the convergence rate. In our previous paper [24], we further analyzed the classical SWR algorithms, where the reaction diffusion equations with a constant delay were considered as the underlying model problems and the convergence behavior of the SWR algorithms with arbitrary number of subdomains is highlighted. For the transmission conditions of Robin type, Vandewalle and Gander [22] proposed a very technical idea to determine the best parameter. However, the details of their idea are not presented in that paper. Therefore, the convergence behavior of the SWR algorithms with Robin transmission conditions for PDEs with time delay has not been fully investigated yet, which is still open and remains challenging.

Following the spirit of [22], in this paper we continue to study the optimized SWR algorithms for PDEs with time delay. By using the reaction diffusion equations with a constant delay as the underlying model problems, we investigate here how to determine the parameter involved in the transmission conditions as better as possible. We establish an algebraic analysis method to determine the quasi-optimized parameter, which is different from the geometrical method given in [22]. Moreover, for the heat equation with a constant delay, we show that the new method results in better parameter involved in the Robin type transmission conditions.

The remainder of this paper is organized as follows. In Section 2, we introduce the used model equations and the SWR algorithms with transmission conditions of Robin type. The well-posedness of the algorithm is proved in this section. Our main results are presented in Section 3, where the optimization problem arising from determining the best parameter involved in the Robin transmission conditions is solved in great details. In Section 4, we consider the special case—the heat equations with a constant time delay, and we show that the quasi-optimized parameter obtained in this paper is better than the one given in [22]. In Section 5, we provide several numerical examples to illustrate the effectiveness of our results. Finally in Section 6, we finish this paper with some conclusion remarks.

2. Model problems and the SWR algorithms

We consider the following reaction diffusion equation with a constant time delay as the model problem:

$$\begin{cases} \dfrac{\partial u}{\partial t} - \nu^2 \dfrac{\partial^2 u}{\partial x^2} + a_1 u(x,t) + a_2 u(x,t-\tau) = f(x,t), & (x,t) \in \mathbb{R} \times (0,T), \\ u(x,t) = u_0(x,t), & (x,t) \in \mathbb{R} \times [-\tau, 0], \\ u(\pm\infty, t) = 0, & t \in (0,T), \end{cases} \tag{2.1}$$

where $\tau > 0$, $\nu > 0$ and a_1, a_2 are constants with $a_2 \neq 0$. This equation is also the basic model investigated by [23]. For $\nu = 1$, $a_1 = 0$ and $a_2\tau > 0$, (2.1) reduces to the one discussed in [22]. We decompose the spatial domain $\Omega = \mathbb{R}$ into two overlapping subdomains $\Omega_1 = (-\infty, L]$ and $\Omega_2 = [0, +\infty)$ with $L \geqslant 0$. The SWR algorithms then consist of solving iteratively subproblems on $\Omega_j \times \mathbb{R}^+$, $j = 1, 2$, using as a boundary condition at the interfaces $x = 0$ and $x = L$ the values obtained from the previous iteration. The iterative scheme is thus for iteration index k given by

$$\begin{cases} \dfrac{\partial u_1^k}{\partial t} - \nu^2 \dfrac{\partial^2 u_1^k}{\partial x^2} + a_1 u_1^k(x,t) + a_2 u_1^k(x,t-\tau) = f(x,t), & (x,t) \in \Omega_1 \times (0,T), \\ u_1^k(x,t) = u_0(x,t), & (x,t) \in \Omega_1 \times [-\tau, 0], \\ \mathcal{B}_1 u_1^k(L,t) = \mathcal{B}_1 u_2^{k-1}(L,t), & t \in (0,T), \end{cases} \tag{2.2}$$

and

$$\begin{cases} \dfrac{\partial u_2^k}{\partial t} - \nu^2 \dfrac{\partial^2 u_2^k}{\partial x^2} + a_1 u_2^k(x,t) + a_2 u_2^k(x,t-\tau) = f(x,t), & (x,t) \in \Omega_2 \times (0,T), \\ u_2^k(x,t) = u_0(x,t), & (x,t) \in \Omega_2 \times [-\tau, 0], \\ \mathcal{B}_2 u_2^k(0,t) = \mathcal{B}_2 u_1^{k-1}(0,t), & t \in (0,T), \end{cases} \tag{2.3}$$

where u_1^0 and u_2^0 are initial guesses, and $\mathcal{B}_1, \mathcal{B}_2$ denote the Robin type transmission conditions:

$$\mathcal{B}_1 = \frac{\partial}{\partial x} + \frac{p}{\nu}, \qquad \mathcal{B}_2 = \frac{\partial}{\partial x} - \frac{p}{\nu} \tag{2.4}$$

with p a free parameter.

We next show the well-posedness of each subdomain problem. We consider this problem in anisotropic Sobolev spaces $H^{r,s}(\Omega \times (0,T)) = L^2(H^r(\Omega); (0,T)) \cap H^s(L^2(\Omega); (0,T))$ where $(0,T)$ denotes the time intervals; see [16]. Without loss of generality, we consider the following subdomain problem on $\Omega_1 \times (0,T)$ only:

$$\begin{cases} \dfrac{\partial w}{\partial t} - \nu^2 \dfrac{\partial^2 w}{\partial x^2} + a_1 w(x,t) + a_2 w(x,t-\tau) = f(x,t), & \text{on } \Omega_1 \times (0,T), \\ w(x,t) = w_0(x,t), & \text{on } \Omega_1 \times [-\tau, 0], \\ \mathcal{B}_1 w(L,t) = g(t), & t \in (0,T). \end{cases} \tag{2.5}$$

Lemma 2.1. *(See [14, Theorem 5.5].) For the following equation*

$$\begin{cases} \dfrac{\partial \tilde{w}}{\partial t} - \nu^2 \dfrac{\partial^2 \tilde{w}}{\partial x^2} + a_1 \tilde{w}(x,t) = \tilde{f}(x,t), & (x,t) \in \Omega_1 \times (0,T), \\ \tilde{w}(x,0) = \tilde{w}_0(x), & x \in \Omega_1, \\ \left(\dfrac{\partial}{\partial x} + \dfrac{p}{\nu} \right) \tilde{w}(L,t) = g(t), & t \in (0,T), \end{cases} \tag{2.6}$$

if $a_1 > 0$, $p \geqslant 0$, $\tilde{f} \in H^{1,\frac{1}{2}}(\Omega_1 \times (0,T))$, $\tilde{w}_0(x) \in H^2(\Omega_1)$, $g(t) \in H^{\frac{3}{4}}(0,T)$, and the compatibility condition

$$\frac{\partial \tilde{w}_0(L)}{\partial x} + \frac{p}{\nu} \tilde{w}_0(L) = g(0)$$

is satisfied, then the solution $\tilde{w}(x,t)$ of (2.6) is in $H^{3,\frac{3}{2}}(\Omega_1 \times (0,T))$. Moreover, the following compatibility property holds at $x = 0$:

$$\lim_{t \to 0+} \left(\frac{\partial}{\partial x} \tilde{w} + \frac{p}{\nu} \tilde{w} \right)(0,t) = \frac{\partial}{\partial x} \tilde{w}_0(0) + \frac{p}{\nu} \tilde{w}_0(0).$$

Lemma 2.2. *Assume $a_1 > 0$, $p \geqslant 0$, $f \in H^{1,\frac{1}{2}}(\Omega_1 \times (0,T))$, $w_0(x,t) \in H^{3,\frac{3}{2}}(\Omega_1 \times (-\tau, 0))$, $g(t) \in H^{\frac{3}{4}}(0,T)$ and the following compatibility property holds*

$$\frac{\partial w_0(L,0)}{\partial x} + \frac{p}{\nu} w_0(L,0) = g(0). \tag{2.7}$$

Then the solution $w(x,t)$ of (2.5) is in $H^{3,\frac{3}{2}}(\Omega_1 \times (0,T))$. Moreover, the following compatibility property holds at $x = 0$:

$$\lim_{t \to 0+} \left(\frac{\partial}{\partial x} w + \frac{p}{\nu} w \right)(0,t) = \frac{\partial}{\partial x} w_0(0,0) + \frac{p}{\nu} w_0(0,0).$$

Proof. In subinterval $[0,\tau]$, (2.5) takes the form of (2.6) with $\tilde{f} = a_2 w_0(x, t-\tau) + f(x,t) \in H^{1,\frac{1}{2}}(\Omega_1 \times (0,\tau))$, and $\tilde{w}_0(x) = w_0(x,0)$. By the trace theorem (see Theorem 3 in [17]), we know that $w_0(x,0) \in H^2(\Omega_1)$ since $w_0(x,t) \in H^{3,\frac{3}{2}}(\Omega_1 \times (-\tau, 0))$. Hence, by the compatibility condition (2.7) and Lemma 2.1, the solution of (2.5)—denoted by $w_\tau(x,t)$, is in $H^{3,\frac{3}{2}}(\Omega_1 \times (0,\tau))$. Moreover, w_τ satisfies

$$w_\tau(x,\tau) \in H^2(\Omega_1) \quad \text{and} \quad \lim_{t \to 0+} \left(\frac{\partial}{\partial x} w_\tau + \frac{p}{\nu} w_\tau \right)(0,t) = \frac{\partial}{\partial x} w_0(0,0) + \frac{p}{\nu} w_0(0,0).$$

Similarly, in the next subinterval $[\tau, 2\tau]$, by using the boundary condition $(\frac{\partial}{\partial x} w_\tau + \frac{p}{\nu} w_\tau)(L,\tau) = g(\tau)$ and Lemma 2.1, we know that there exists a solution—denoted by $w_{2\tau}(x,t)$, of (2.5) in $H^{3,\frac{3}{2}}(\Omega_1 \times (\tau, 2\tau))$. Therefore, by a simple induction technique, we can obtain a unique solution $w(x,t)$ of (2.5) in $H^{3,\frac{3}{2}}(\Omega_1 \times (0,T))$ with $\lim_{t \to 0+} (\frac{\partial}{\partial x} w + \frac{p}{\nu} w)(0,t) = \frac{\partial}{\partial x} w_0(0,0) + \frac{p}{\nu} w_0(0,0)$. □

By using Lemma 2.2 and induction rule, we can prove the well-posedness of the SWR algorithm (2.2)–(2.4).

Theorem 2.1. *Assume $a > 0$, $p \geqslant 0$, $u_0(x,t) \in H^{3,\frac{3}{2}}(\mathbb{R}\times[0,-\tau])$ and $f \in H^{1,\frac{1}{2}}(\mathbb{R}\times\mathbb{R}^+)$. Let g_0, g_L be given in $H^{\frac{3}{4}}(\mathbb{R}^+)$ and the initial guesses u_1^0, u_2^0 of the SWR algorithm (2.2)–(2.4) satisfy $(\frac{\partial}{\partial x}u_1^0 + \frac{p}{\nu}u_1^0)(L,t) = g_L(t)$ and $(\frac{\partial}{\partial x}u_2^0 + \frac{p}{\nu}u_2^0)(0,t) = g_0(t)$. Then, algorithm (2.2)–(2.4) defines a sequence of iterates (u_1^k, u_2^k) in $H^{3,\frac{3}{2}}(\Omega_1\times\mathbb{R}^+)\times H^{3,\frac{3}{2}}(\Omega_2\times\mathbb{R}^+)$.*

3. Towards the best parameter of p

In this section, we focus on determining the best choice of parameter p in the transmission conditions (2.4). We consider the case $T = +\infty$, i.e., the SWR algorithm (2.2)–(2.4) is implemented on sufficient long time intervals. Let e_k^j be the errors on subdomain Ω_j $(j = 1, 2)$ at iteration $k \geqslant 0$, i.e.,

$$e_k^1 = u|_{\Omega_1} - u_k^1, \qquad e_k^2 = u|_{\Omega_2} - u_k^2.$$

Then the homogeneous error equations for the SWR iterations (2.2)–(2.4) are

$$\begin{cases} \dfrac{\partial e_k^1}{\partial t} - \nu^2\dfrac{\partial^2 e_k^1}{\partial x^2} + a_1 e_k^1(x,t) + a_2 e_k^1(x,t-\tau) = 0, & (x,t)\in\Omega_1\times\mathbb{R}^+, \\ e_k^1(x,t) = 0, & (x,t)\in\Omega_1\times(-\tau,0), \\ \left(\dfrac{\partial}{\partial x} + \dfrac{p}{\nu}\right)e_k^1(L,t) = \left(\dfrac{\partial}{\partial x} + \dfrac{p}{\nu}\right)e_{k-1}^2(L,t), & t\in\mathbb{R}^+, \end{cases} \tag{3.1a}$$

and

$$\begin{cases} \dfrac{\partial e_k^2}{\partial t} - \nu^2\dfrac{\partial^2 e_k^2}{\partial x^2} + a_1 e_k^2(x,t) + a_2 e_k^2(x,t-\tau) = 0, & (x,t)\in\Omega_2\times\mathbb{R}^+, \\ e_k^2(x,0) = 0, & (x,t)\in\Omega_2\times(-\tau,0), \\ \left(\dfrac{\partial}{\partial x} - \dfrac{p}{\nu}\right)e_k^2(0,t) = \left(\dfrac{\partial}{\partial x} - \dfrac{p}{\nu}\right)e_{k-1}^1(0,t), & t\in\mathbb{R}^+. \end{cases} \tag{3.1b}$$

We perform the Fourier transform in time of the error equations (3.1), and this gives

$$\begin{cases} \dfrac{\partial^2\hat{e}_k^1(x,\omega)}{\partial x^2} - \dfrac{a_1 + a_2 e^{-i\omega\tau} + i\omega}{\nu^2}\hat{e}_k^1(x,\omega) = 0, \\ \left(\dfrac{\partial}{\partial x} + \dfrac{p}{\nu}\right)\hat{e}_k^1(L,\omega) = \left(\dfrac{\partial}{\partial x} + \dfrac{p}{\nu}\right)\hat{e}_{k-1}^2(L,\omega), \end{cases} \tag{3.2a}$$

and

$$\begin{cases} \dfrac{\partial^2\hat{e}_k^2(x,\omega)}{\partial x^2} - \dfrac{a_1 + a_2 e^{-i\omega\tau} + i\omega}{\nu^2}\hat{e}_k^2(x,\omega) = 0, \\ \left(\dfrac{\partial}{\partial x} - \dfrac{p}{\nu}\right)\hat{e}_k^2(0,\omega) = \left(\dfrac{\partial}{\partial x} - \dfrac{p}{\nu}\right)\hat{e}_{k-1}^1(0,\omega), \end{cases} \tag{3.2b}$$

where $\hat{e}_k^j(x,\omega) = \frac{1}{2\pi}\int_{\mathbb{R}} e_k^j(x,t)e^{-i\omega t}\,dt$ (we extend $e_k^j = 0$ for $t < -\tau$ and denote the extension by e_k^j, too), $j = 1, 2$. We are thus led to solve an ordinary differential equation in each subdomain. The roots of the corresponding characteristic polynomial are

$$\lambda_+ = \frac{\sqrt{a_1 + a_2 e^{-i\omega\tau} + i\omega}}{\nu}, \qquad \lambda_- = -\frac{\sqrt{a_1 + a_2 e^{-i\omega\tau} + i\omega}}{\nu}. \tag{3.3}$$

A routine calculation yields

$$\lambda_+ = \frac{\xi(\omega) + i\psi(\omega)}{\nu}, \qquad \lambda_- = -\frac{\xi(\omega) + i\psi(\omega)}{\nu}, \tag{3.4}$$

where

$$\begin{aligned} \xi(\omega) &= \sqrt{\frac{a_1 + a_2\cos(\omega\tau) + \sqrt{(a_1 + a_2\cos(\omega\tau))^2 + (\omega - a_2\sin(\omega\tau))^2}}{2}}, \\ \psi(\omega) &= \delta\sqrt{\frac{-a_1 - a_2\cos(\omega\tau) + \sqrt{(a_1 + a_2\cos(\omega\tau))^2 + (\omega - a_2\sin(\omega\tau))^2}}{2}}, \end{aligned} \tag{3.5}$$

where $\delta = \operatorname{sign}(\omega - a_2\sin(\omega\tau))$.

Clearly, $\Re(\lambda_+) \geqslant 0$ and $\Re(\lambda_-) \leqslant 0$, and thus the solutions of (3.2) that do not increase exponentially at infinity are

$$\begin{cases} \hat{e}_k^1(x,\omega) = \alpha_k(\omega) e^{\lambda_+(x-L)}, & \text{for } (x,\omega) \in (-\infty, L) \times \mathbb{R}, \\ \hat{e}_k^2(x,\omega) = \beta_k(\omega) e^{\lambda_- x}, & \text{for } (x,\omega) \in (0, +\infty) \times \mathbb{R}, \end{cases} \tag{3.6}$$

where $\alpha_k(\omega)$ and $\beta_k(\omega)$ will be computed with the boundary conditions on $x = L$ and $x = 0$:

$$\alpha_k(\omega) = \frac{(\lambda_- + \frac{p}{\nu}) e^{\lambda_- L}}{\lambda_+ + \frac{p}{\nu}} \beta_{k-1}(\omega), \qquad \beta_k(\omega) = \frac{(\lambda_+ - \frac{p}{\nu}) e^{-\lambda_+ L}}{\lambda_- - \frac{p}{\nu}} \alpha_{k-1}(\omega). \tag{3.7}$$

Hence, the errors $\hat{e}_k^j(x,\omega)$ $(j = 1, 2)$ satisfy

$$\hat{e}_k^j(x,\omega) = \frac{(\lambda_- + \frac{p}{\nu})(\lambda_+ - \frac{p}{\nu})}{(\lambda_+ + \frac{p}{\nu})(\lambda_- - \frac{p}{\nu})} e^{(\lambda_- - \lambda_+)L} \hat{e}_{k-2}^j(x,\omega), \quad j = 1, 2. \tag{3.8}$$

By these relations and the well-known Parseval–Plancherel identity we get

$$\left\| e_k^1 \right\|_{L^2} \leqslant \rho(p, L) \left\| e_{k-2}^1 \right\|_{L^2}, \qquad \left\| e_k^2 \right\|_{L^2} \leqslant \rho(p, L) \left\| e_{k-2}^2 \right\|_{L^2}, \tag{3.9}$$

where $\rho(p, L)$ is the convergence factor of the SWR algorithm (2.2)–(2.4) and will be defined later.

We note that in a numerical computation, a numerical grid in time with spacing Δt cannot carry arbitrary high frequencies—this means that the quantity ω in λ_- and λ_+ cannot vary from $-\infty$ to $+\infty$; an estimate of the highest frequency is $\omega_{\max} = \frac{\pi}{\Delta t}$ (see [14]). Therefore, the convergence factor $\rho(p, L)$ in (3.9) should be defined by

$$\rho(p, L) = \max_{\omega \in [-\omega_{\max}, \omega_{\max}]} \left| \frac{(\lambda_- + \frac{p}{\nu})(\lambda_+ - \frac{p}{\nu})}{(\lambda_+ + \frac{p}{\nu})(\lambda_- - \frac{p}{\nu})} e^{(\lambda_- - \lambda_+)L} \right|. \tag{3.10}$$

Hence, the best constant p involved in the transmission condition of Robin type should be determined by the following min–max problem:

$$\min_{p>0} \max_{\omega \in [-\omega_{\max}, \omega_{\max}]} \left| \frac{(\lambda_- + \frac{p}{\nu})(\lambda_+ - \frac{p}{\nu})}{(\lambda_+ + \frac{p}{\nu})(\lambda_- - \frac{p}{\nu})} e^{(\lambda_- - \lambda_+)L} \right|. \tag{3.11}$$

We next show that this is a complex problem and is essentially different from the regular cases studied in [1,14]. By (3.3) and (3.10) we know that the convergence factor ρ can be rewritten as

$$\rho(p, L) = \max_{z \in \Gamma} \left| \frac{(z-p)^2}{(z+p)^2} e^{-2\frac{z}{\nu}L} \right|, \tag{3.12a}$$

where

$$\Gamma = \left\{ z\colon\ z = \sqrt{a_1 + i\omega + a_2 e^{-i\omega\tau}},\ \omega \in [-\omega_{\max}, \omega_{\max}] \right\}. \tag{3.12b}$$

Clearly, for $\tau = 0$ we have $\Gamma = \{z\colon\ z = \sqrt{(a_1 + a_2) + i\omega},\ \omega \in [-\omega_{\max}, \omega_{\max}]\}$, which is obviously a simple curve in the complex plane (see Fig. 3.1). However, for $\tau \neq 0$, the curve Γ is complex which can be seen in Fig. 3.2, where $a_1 = 1.5$, $a_2 = -1$ and $\tau = 1.5, 3$ are considered. For $L = 0$, $\nu = 1$ and $a_1 = 0$, Vandewalle and Gander [22] proposed that:

1. Choose a regular *box* (denoted by $\mathbb{B}$) which contains the curve Γ; see the sketch map in Fig. 3.3;
2. Solve the following min–max problem instead of (3.11) with $L = 0$:

$$\min_{p>0} \max_{z \in \mathbb{B}} \left| \frac{(z-p)^2}{(z+p)^2} \right|. \tag{3.13}$$

Clearly, the solution of (3.13) is a quasi-optimized solution of the min–max problem (3.11) with $L = 0$. It is a pity that we have not found the details about how to choose the box $\mathbb{B}$ and how to solve the min–max problem in the bounding box $\mathbb{B}$. In this paper, we continue to consider the case $L = 0$ and try to derive a better quasi-optimized solution of the min–max problem (3.11).

Remark 3.1. The homogeneous error equations (3.1a)–(3.1b) can be equivalently written as

$$\begin{cases} \dfrac{\partial e_k^1}{\partial t} - \nu^2 \dfrac{\partial^2 e_k^1}{\partial x^2} + a_1 e_k^1(x,t) + a_2 e_k^1(x, t-\tau) = 0, & (x,t) \in \Omega_1 \times \mathbb{R}^+, \\ e_k^1(x,t) = 0, & (x,t) \in \Omega_1 \times (-\tau, 0), \\ \left(\dfrac{1}{p} \dfrac{\partial}{\partial x} + \dfrac{1}{\nu} \right) e_k^1(L,t) = \left(\dfrac{1}{p} \dfrac{\partial}{\partial x} + \dfrac{1}{\nu} \right) e_{k-1}^2(L,t), & t \in \mathbb{R}^+, \end{cases}$$

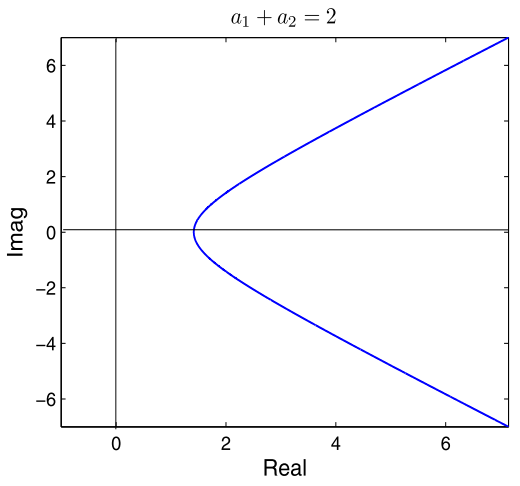

Fig. 3.1. The curve Γ for $\tau = 0$ and $a_1 + a_2 = 2$.

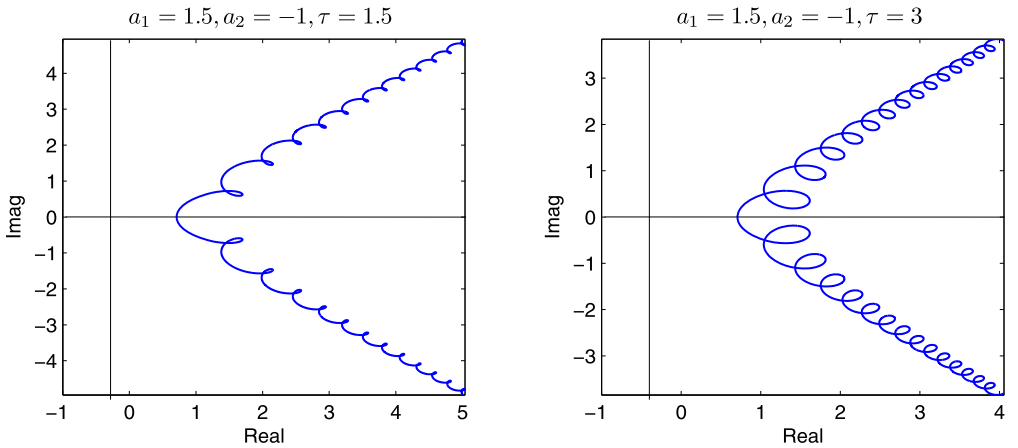

Fig. 3.2. The curve Γ for $a_1 = 1.5$, $a_2 = -1$ and $\tau = 1.5$ (left), $\tau = 3$ (right).

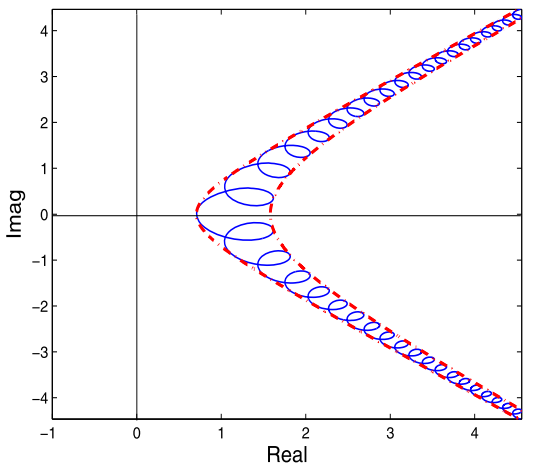

Fig. 3.3. Sketch map of the curve Γ (solid line) and the box $\mathbb{B}$ (dash–dot line).

and

$$\begin{cases} \dfrac{\partial e_k^2}{\partial t} - \nu^2 \dfrac{\partial^2 e_k^2}{\partial x^2} + a_1 e_k^2(x,t) + a_2 e_k^2(x,t-\tau) = 0, & (x,t) \in \Omega_2 \times \mathbb{R}^+, \\ e_k^2(x,0) = 0, & (x,t) \in \Omega_2 \times (-\tau, 0), \\ \left(\dfrac{1}{p}\dfrac{\partial}{\partial x} - \dfrac{1}{\nu}\right) e_k^2(0,t) = \left(\dfrac{1}{p}\dfrac{\partial}{\partial x} - \dfrac{1}{\nu}\right) e_{k-1}^1(0,t), & t \in \mathbb{R}^+. \end{cases}$$

Then, by letting $p \to +\infty$ we get

$$\begin{cases} \dfrac{\partial e_k^1}{\partial t} - \nu^2 \dfrac{\partial^2 e_k^1}{\partial x^2} + a_1 e_k^1(x,t) + a_2 e_k^1(x,t-\tau) = 0, & (x,t) \in \Omega_1 \times \mathbb{R}^+, \\ e_k^1(x,t) = 0, & (x,t) \in \Omega_1 \times (-\tau, 0), \\ e_k^1(L,t) = e_{k-1}^2(L,t), & t \in \mathbb{R}^+, \end{cases}$$

and

$$\begin{cases} \dfrac{\partial e_k^2}{\partial t} - \nu^2 \dfrac{\partial^2 e_k^2}{\partial x^2} + a_1 e_k^2(x,t) + a_2 e_k^2(x,t-\tau) = 0, & (x,t) \in \Omega_2 \times \mathbb{R}^+, \\ e_k^2(x,0) = 0, & (x,t) \in \Omega_2 \times (-\tau, 0), \\ e_k^2(0,t) = e_{k-1}^1(0,t), & t \in \mathbb{R}^+, \end{cases}$$

which corresponds to the error equations for the SWR iterations (2.2)–(2.3) with Dirichlet transmission conditions—$\mathcal{B}_1 = \mathcal{B}_2 = \mathcal{I}$, where $\mathcal{I}$ denotes the identity operator. Hence, by letting $p \to +\infty$ in (3.10) we get the convergence factor of the SWR algorithms with Dirichlet transmission conditions

$$\rho_{\mathrm{Dir}} := \max_{\omega \in [-\omega_{\max}, \omega_{\max}]} \left| e^{(\lambda_- - \lambda_+)L} \right|.$$

Clearly, $\rho_{\mathrm{Dir}} = 1$ if $L = 0$. This means that $L > 0$ is necessary to theoretically guarantee the convergence of the SWR algorithms with Dirichlet transmission conditions. However, as we will show in the sequel that for $L = 0$ the SWR algorithms with Robin transmission conditions can be convergent with satisfactory convergence rate by properly choosing the parameter p (see the results shown in Fig. 4.2).

To solve the min–max problem (3.13) with $L = 0$, we first rewrite $\rho(p,0)$ in (3.12a)–(3.12b) as

$$\rho(p,0) = \max_{\omega \in [-\omega_{\max}, \omega_{\max}]} \left| \frac{[\xi(\omega) + i\psi(\omega) - p]^2}{[\xi(\omega) + i\psi(\omega) + p]^2} \right| = \max_{\omega \in [-\omega_{\max}, \omega_{\max}]} \frac{(\xi(\omega) - p)^2 + \psi^2(\omega)}{(\xi(\omega) + p)^2 + \psi^2(\omega)}, \tag{3.14}$$

where $\xi(\omega)$ and $\psi(\omega)$ are defined by (3.5). Since $\xi^2(\omega) - \psi^2(\omega) = a_1 + a_2\cos(\omega\tau)$, we get from (3.14) that

$$\rho(p,0) = \max_{\omega \in [-\omega_{\max}, \omega_{\max}]} \frac{(\xi(\omega) - p)^2 + \xi^2(\omega) - a_1 - a_2\cos(\omega\tau)}{(\xi(\omega) + p)^2 + \xi^2(\omega) - a_1 - a_2\cos(\omega\tau)}. \tag{3.15}$$

Define

$$\begin{aligned} &\zeta_0 = \min_{\omega \in [-\omega_{\max}, \omega_{\max}]} \xi(\omega), \qquad \zeta_1 = \max_{\omega \in [-\omega_{\max}, \omega_{\max}]} \xi(\omega), \\ &\hat{\rho}(p,0) = \max_{\zeta \in [\zeta_0, \zeta_1], s \in [-1,1]} \frac{(\zeta - p)^2 + \zeta^2 - a_1 + |a_2|s}{(\zeta + p)^2 + \zeta^2 - a_1 + |a_2|s}. \end{aligned} \tag{3.16}$$

Then, it is clear that

$$\rho(p,0) \leqslant \hat{\rho}(p,0). \tag{3.17}$$

Moreover, for any $\zeta \in [\zeta_0, \zeta_1]$ it is easy to get

$$\max_{s \in [-1,1]} \frac{(\zeta - p)^2 + \zeta^2 - a_1 + |a_2|s}{(\zeta + p)^2 + \zeta^2 - a_1 + |a_2|s} = \frac{(\zeta - p)^2 + \zeta^2 - a_1 + |a_2|}{(\zeta + p)^2 + \zeta^2 - a_1 + |a_2|}, \tag{3.18}$$

since $|a_2| > 0$. Therefore, $\hat{\rho}(p,0) = \max_{\zeta \in [\zeta_0, \zeta_1]} \frac{(\zeta - p)^2 + \zeta^2 - a_1 + |a_2|}{(\zeta + p)^2 + \zeta^2 - a_1 + |a_2|}$. Hence, from (3.17) we have

$$\min_{p>0} \rho(p,0) \leqslant \min_{p>0} \left(\max_{\zeta \in [\zeta_0, \zeta_1]} \frac{(\zeta - p)^2 + \zeta^2 - a_1 + |a_2|}{(\zeta + p)^2 + \zeta^2 - a_1 + |a_2|} \right). \tag{3.19}$$

Let

$$\tilde{\alpha} = a_1 - |a_2|, \qquad \tilde{R}(\zeta, p, \tilde{\alpha}) = \frac{(\zeta - p)^2 + \zeta^2 - \tilde{\alpha}}{(\zeta + p)^2 + \zeta^2 - \tilde{\alpha}}. \tag{3.20}$$

Then by using (3.19) we have

$$\min_{p>0} \rho(p, 0) \leqslant \min_{p>0}\Big(\max_{\zeta \in [\zeta_0, \zeta_1]} \tilde{R}(\zeta, p, \tilde{\alpha})\Big). \tag{3.21}$$

Lemma 3.1. *The quantities $\tilde{\alpha}$ and ζ_0 satisfy $\zeta_0^2 \geqslant \tilde{\alpha}$.*

Proof. By the definitions of $\tilde{\alpha}$ and ζ_0, it is sufficient to prove $\xi^2(\omega) \geqslant a_1 - |a_2|$ for all $\omega \in \mathbb{R}$, since $\zeta_0 = \min_{\omega \in [-\omega_{\max}, \omega_{\max}]} \xi(\omega)$. Straightforward calculations yield

$$\begin{aligned}
\xi^2(\omega) - \big(a_1 - |a_2|\big) &= \frac{\sqrt{[a_1 + a_2\cos(\omega\tau)]^2 + [\omega - a_2\sin(\omega\tau)]^2} + a_1 + a_2\cos(\omega\tau)}{2} - a_1 + |a_2| \\
&= \frac{\sqrt{[a_1 + a_2\cos(\omega\tau)]^2 + [\omega - a_2\sin(\omega\tau)]^2} - a_1 + 2|a_2| + a_2\cos(\omega\tau)}{2} \\
&\geqslant \frac{\sqrt{[a_1 + a_2\cos(\omega\tau)]^2 + [\omega - a_2\sin(\omega\tau)]^2} - a_1 - a_2\cos(\omega\tau)}{2} \\
&\geqslant 0,
\end{aligned} \tag{3.22}$$

which completes the proof. □

Remark 3.2. For regular reaction diffusion equations, for example $a_2 = 0$ and $a_1 > 0$, it is easy to get $\zeta_0 = \sqrt{a_1}$ and $\tilde{\alpha} = \zeta_0^2$. In this case, the problem $\min_{p>0}(\max_{\zeta \in [\zeta_0, \zeta_1]} \tilde{R}(\zeta, p, \zeta_0^2))$ can be solved in closed formulas and the interested reader can refer to the work by Gander et al. [1,14]. However, if time delay is involved, i.e., $\tau > 0$ and $a_2 \neq 0$, we know from Lemma 3.1 that $\tilde{\alpha} \leqslant \zeta_0^2$, which means that we need to solve a more general min–max problem than the regular case.

In what follows, we try to solve the min–max problem in the right-hand side of (3.21), and the solution can be regarded as a quasi-optimized parameter of $\min_{p>0} \rho(p, 0)$.

Theorem 3.1. *Assume $\zeta_0 > 0$. Then the best parameter which solves the following min–max problem*

$$\min_{p>0}\Big(\max_{\zeta \in [\zeta_0, \zeta_1]} \tilde{R}(\zeta, p, \tilde{\alpha})\Big) \tag{3.23}$$

is determined as

$$p^* = \sqrt{2\zeta_0\zeta_1 + \tilde{\alpha}}, \tag{3.24a}$$

if $\zeta_0^2 - \zeta_0\zeta_1 - \tilde{\alpha} \leqslant 0$ and $\zeta_1^2 - \zeta_0\zeta_1 - \tilde{\alpha} \geqslant 0$; otherwise,

$$p^* = \begin{cases} \sqrt{2\zeta_0^2 - \tilde{\alpha}}, & \text{if } \tilde{R}(\zeta_0, \sqrt{2\zeta_0^2 - \tilde{\alpha}}, \tilde{\alpha}) \geqslant \tilde{R}(\zeta_1, \sqrt{2\zeta_0^2 - \tilde{\alpha}}, \tilde{\alpha}), \\ \sqrt{2\zeta_1^2 - \tilde{\alpha}}, & \text{if } \tilde{R}(\zeta_0, \sqrt{2\zeta_0^2 - \tilde{\alpha}}, \tilde{\alpha}) < \tilde{R}(\zeta_1, \sqrt{2\zeta_0^2 - \tilde{\alpha}}, \tilde{\alpha}). \end{cases} \tag{3.24b}$$

With parameter p^*, the convergence factor ρ can be bounded by

$$\rho\big(p^*, 0\big) \leqslant \begin{cases} \frac{(\zeta_0 - p^*)^2 + \zeta_0^2 - \tilde{\alpha}}{(\zeta_0 + p^*)^2 + \zeta_0^2 - \tilde{\alpha}}, & \text{if } \tilde{R}(\zeta_0, \sqrt{2\zeta_0^2 - \tilde{\alpha}}, \tilde{\alpha}) \geqslant \tilde{R}(\zeta_1, \sqrt{2\zeta_0^2 - \tilde{\alpha}}, \tilde{\alpha}), \\ & \quad \zeta_0^2 - \zeta_0\zeta_1 - \tilde{\alpha} > 0 \text{ or } \zeta_1^2 - \zeta_0\zeta_1 - \tilde{\alpha} < 0, \\ \frac{(\zeta_1 - p^*)^2 + \zeta_1^2 - \tilde{\alpha}}{(\zeta_1 + p^*)^2 + \zeta_1^2 - \tilde{\alpha}}, & \text{otherwise}. \end{cases} \tag{3.25}$$

Proof. For any $\zeta \in [\zeta_0, \zeta_1]$, it is easy to get

$$\frac{\partial \tilde{R}(\zeta, p, \tilde{\alpha})}{\partial p} = 4\zeta \frac{p^2 - 2\zeta^2 + \tilde{\alpha}}{[(\zeta + p)^2 + \zeta^2 - \tilde{\alpha}]^2}. \tag{3.26}$$

Hence, the best parameter p^* shall satisfies $\sqrt{2\zeta_0^2-\tilde{\alpha}} \leqslant p^* \leqslant \sqrt{2\zeta_1^2-\tilde{\alpha}}$. Otherwise, if $p \in (0, \sqrt{2\zeta_0^2-\tilde{\alpha}})$, we have $\partial_p \tilde{R}(\zeta, p, \tilde{\alpha}) < 0$ and therefore increasing p will decrease $\tilde{R}$. Similarly, if $p > \sqrt{2\zeta_1^2-\tilde{\alpha}}$, we have $\partial_p \tilde{R}(\zeta, p, \tilde{\alpha}) > 0$, which means that decreasing p will decrease $\tilde{R}$.

For any $p \in [\sqrt{2\zeta_0^2-\tilde{\alpha}}, \sqrt{2\zeta_1^2-\tilde{\alpha}}]$, we state the following three conclusions.

(a) $\tilde{R}$ does not have local maximum in the interior of the interval $[\zeta_0, \zeta_1]$. By the contrary, there exists some $\zeta^* \in (\zeta_0, \zeta_1)$ such that $\frac{\partial \tilde{R}(\zeta^*, p, \tilde{\alpha})}{\partial \zeta} = 0$, i.e., $\zeta^* = \sqrt{\frac{p^2-\tilde{\alpha}}{2}}$, since

$$\frac{\partial \tilde{R}(\zeta, p, \tilde{\alpha})}{\partial \zeta} = 4p \frac{2\zeta^2 - p^2 + \tilde{\alpha}}{[(\zeta+p)^2 + \zeta^2 - \tilde{\alpha}]^2}. \tag{3.27}$$

On the other hand, a straightforward calculation yields

$$\frac{\partial^2 \tilde{R}(\zeta, p, \tilde{\alpha})}{\partial \zeta^2} = 16p \frac{D(\zeta)}{[(\zeta+p)^2 + \zeta^2 - \tilde{\alpha}]^3}, \tag{3.28}$$

where

$$D(\zeta) = -2\zeta^3 + 3\big(p^2 - \tilde{\alpha}\big)\zeta + p\big(p^2 - \tilde{\alpha}\big). \tag{3.29}$$

It is easy to get

$$D\big(\zeta^*\big) = -2\left(\sqrt{\frac{p^2-\tilde{\alpha}}{2}}\right)^3 + 3\big(p^2-\tilde{\alpha}\big)\left(\sqrt{\frac{p^2-\tilde{\alpha}}{2}}\right) + p\big(p^2-\tilde{\alpha}\big) = \big(p^2-\tilde{\alpha}\big)\left(2\sqrt{\frac{p^2-\tilde{\alpha}}{2}} + p\right). \tag{3.30}$$

Moreover, since $\zeta^* \in (\zeta_0, \zeta_1)$, it shall holds $\sqrt{\frac{p^2-\tilde{\alpha}}{2}} > \zeta_0$, i.e., $p^2 > 2\zeta_0^2 + \tilde{\alpha}$, which gives $p^2 - \tilde{\alpha} > 0$ since $\zeta_0 > 0$. By (3.30) we get $D(\zeta^*) > 0$ and this means $\frac{\partial^2 \tilde{R}(\zeta, p, \tilde{\alpha})}{\partial \zeta^2}|_{\zeta=\zeta^*} > 0$. Hence, $\zeta = \zeta^*$ is not a local maximum point of $\tilde{R}$, but a local minimum point. Therefore,

$$\min_{p>0}\Big(\max_{\zeta\in[\zeta_0,\zeta_1]} \tilde{R}(\zeta, p, \tilde{\alpha})\Big) = \min_{p>0}\big\{\tilde{R}(\zeta_0, p, \tilde{\alpha}), \tilde{R}(\zeta_1, p, \tilde{\alpha})\big\}. \tag{3.31}$$

(b) $\tilde{R}(\zeta_0, p, \tilde{\alpha})$ and $\tilde{R}(\zeta_1, p, \tilde{\alpha})$ have a unique intersection point

$$\bar{p}^* = \sqrt{2\zeta_0\zeta_1 + \tilde{\alpha}},$$

provided $2\zeta_0\zeta_1 + \tilde{\alpha} \geqslant 2\zeta_0^2 - \tilde{\alpha}$, i.e.,

$$\zeta_0^2 - \zeta_0\zeta_1 - \tilde{\alpha} \leqslant 0. \tag{3.32}$$

(c) $\tilde{R}(\zeta_0, p, \tilde{\alpha})$ increases and $\tilde{R}(\zeta_1, p, \tilde{\alpha})$ decreases with respect to p, respectively. This can be deduced from (3.26) straightforwardly.

We next consider the following three cases.

Case 1: $\zeta_0^2 - \zeta_0\zeta_1 - \tilde{\alpha} > 0$. In this case, $\tilde{R}(\zeta_0, p, \tilde{\alpha})$ and $\tilde{R}(\zeta_1, p, \tilde{\alpha})$ do not intersect. Hence, for any $p \in [\sqrt{2\zeta_0^2-\tilde{\alpha}}\sqrt{2\zeta_1^2-\tilde{\alpha}}]$, by the monotonicity of $\tilde{R}(\zeta_0, p, \tilde{\alpha})$ and $\tilde{R}(\zeta_1, p, \tilde{\alpha})$, we know

$$\begin{cases} \tilde{R}(\zeta_0, p, \tilde{\alpha}) \leqslant \tilde{R}(\zeta_1, p, \tilde{\alpha}), & \text{if } \tilde{R}(\zeta_0, \sqrt{2\zeta_0^2-\tilde{\alpha}}, \tilde{\alpha}) < \tilde{R}(\zeta_1, \sqrt{2\zeta_0^2-\tilde{\alpha}}, \tilde{\alpha}), \\ \tilde{R}(\zeta_0, p, \tilde{\alpha}) \geqslant \tilde{R}(\zeta_1, p, \tilde{\alpha}), & \text{otherwise.} \end{cases} \tag{3.33}$$

The above two situations are illustrated in Fig. 3.4. Therefore, $\forall p \in [\sqrt{2\zeta_0^2-\tilde{\alpha}}, \sqrt{2\zeta_1^2-\tilde{\alpha}}]$, we get

$$\max_{\zeta\in[\zeta_0,\zeta_1]} \tilde{R}(\zeta, p, \tilde{\alpha}) = \begin{cases} \tilde{R}(\zeta_1, p, \tilde{\alpha}), & \text{if } \tilde{R}(\zeta_0, \sqrt{2\zeta_0^2-\tilde{\alpha}}, \tilde{\alpha}) < \tilde{R}(\zeta_1, \sqrt{2\zeta_0^2-\tilde{\alpha}}, \tilde{\alpha}), \\ \tilde{R}(\zeta_0, p, \tilde{\alpha}), & \text{otherwise.} \end{cases} \tag{3.34}$$

Therefore, by using the monotonicity of $\tilde{R}(\zeta_0, p, \tilde{\alpha})$ and $\tilde{R}(\zeta_1, p, \tilde{\alpha})$ again, the solution of the min–max problem (3.23) is

$$p^* = \begin{cases} \sqrt{2\zeta_1^2-\tilde{\alpha}}, & \text{if } \tilde{R}(\zeta_0, \sqrt{2\zeta_0^2-\tilde{\alpha}}, \tilde{\alpha}) < \tilde{R}(\zeta_1, \sqrt{2\zeta_0^2-\tilde{\alpha}}, \tilde{\alpha}), \\ \sqrt{2\zeta_0^2-\tilde{\alpha}}, & \text{otherwise.} \end{cases} \tag{3.35}$$

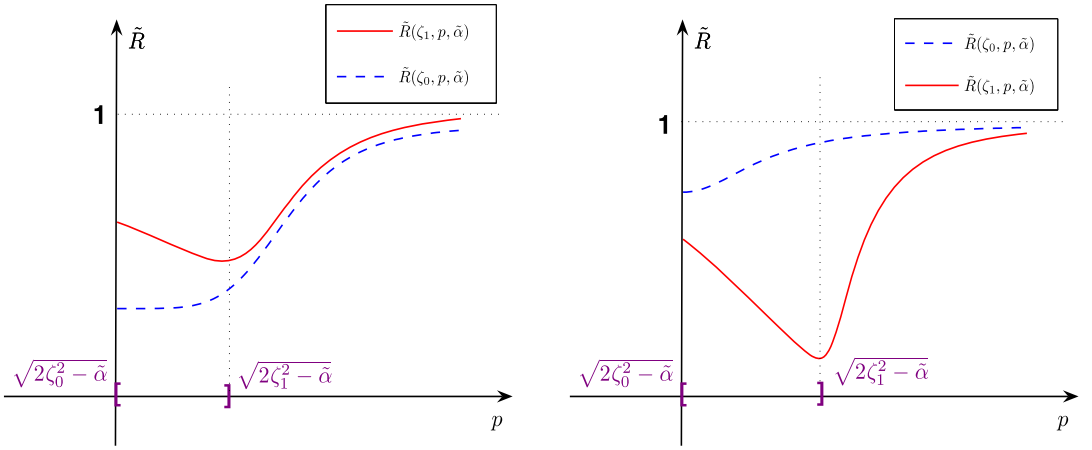

Fig. 3.4. Sketch map of $\tilde{R}(\zeta_0,p,\tilde{\alpha})$ and $\tilde{R}(\zeta_1,p,\tilde{\alpha})$ for $\zeta_0^2-\zeta_0\zeta_1-\tilde{\alpha}>0$. Left: $\tilde{R}(\zeta_0,\sqrt{2\zeta_0^2-\tilde{\alpha}},\tilde{\alpha})<\tilde{R}(\zeta_1,\sqrt{2\zeta_0^2-\tilde{\alpha}})$; Right: $\tilde{R}(\zeta_0,\sqrt{2\zeta_0^2-\tilde{\alpha}},\tilde{\alpha})\geqslant\tilde{R}(\zeta_1,\sqrt{2\zeta_0^2-\tilde{\alpha}})$.

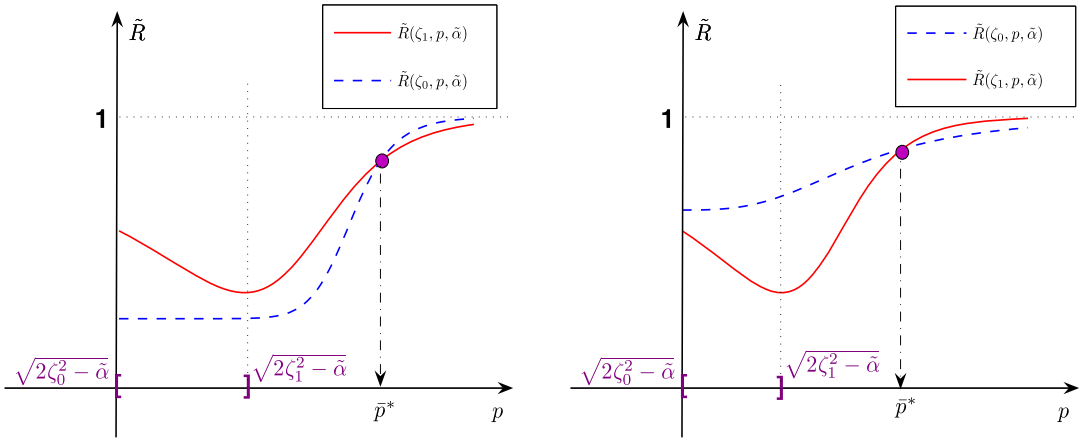

Fig. 3.5. Sketch map of $\tilde{R}(\zeta_0,p,\tilde{\alpha})$ and $\tilde{R}(\zeta_1,p,\tilde{\alpha})$ for $\zeta_0^2-\zeta_0\zeta_1-\tilde{\alpha}\leqslant 0$ and $\zeta_1^2-\zeta_0\zeta_1-\tilde{\alpha}<0$. Left: $\tilde{R}(\zeta_0,\sqrt{2\zeta_0^2-\tilde{\alpha}},\tilde{\alpha})<\tilde{R}(\zeta_1,\sqrt{2\zeta_0^2-\tilde{\alpha}})$; Right: $\tilde{R}(\zeta_0,\sqrt{2\zeta_0^2-\tilde{\alpha}},\tilde{\alpha})\geqslant\tilde{R}(\zeta_1,\sqrt{2\zeta_0^2-\tilde{\alpha}})$.

Case 2: $\zeta_0^2-\zeta_0\zeta_1-\tilde{\alpha}\leqslant 0$ and $\bar{p}^*>\sqrt{2\zeta_1^2-\tilde{\alpha}}$ (i.e., $\zeta_1^2-\zeta_0\zeta_1-\tilde{\alpha}<0$). In this case, $\tilde{R}(\zeta_0,p,\tilde{\alpha})$ and $\tilde{R}(\zeta_1,p,\tilde{\alpha})$ intersect at $p=\bar{p}^*$, which satisfies $\bar{p}^*>\sqrt{2\zeta_1^2-\tilde{\alpha}}$. Therefore, there are two situations that need to be considered as illustrated in Fig. 3.5; the analysis for this case is similar to that of Case 1 and we therefore omit it.

Case 3: $\zeta_0^2-\zeta_0\zeta_1-\tilde{\alpha}\leqslant 0$ and $\bar{p}^*\leqslant\sqrt{2\zeta_1^2-\tilde{\alpha}}$ (i.e., $\zeta_1^2-\zeta_0\zeta_1-\tilde{\alpha}\geqslant 0$). In this case, the unique intersection point $\bar{p}^*$ satisfies

$$\bar{p}^*\in\Big[\sqrt{2\zeta_0^2-\tilde{\alpha}},\sqrt{2\zeta_1^2-\tilde{\alpha}}\Big].$$

Hence, the solution of the min–max problem (3.23) is the point where $\tilde{R}(\zeta_0,p,\tilde{\alpha})$ and $\tilde{R}(\zeta_1,p,\tilde{\alpha})$ are balanced (see the illustration map shown in Fig. 3.6), i.e., $p^*=\bar{p}^*=\sqrt{2\zeta_0\zeta_1+\tilde{\alpha}}$. Moreover, we have

$$\max_{\zeta\in[\zeta_0,\zeta_1]}\tilde{R}\big(\zeta,p^*,\tilde{\alpha}\big)=\tilde{R}\big(\zeta_0,p^*,\tilde{\alpha}\big)=\tilde{R}\big(\zeta_1,p^*,\tilde{\alpha}\big). \tag{3.36}$$

By the analysis of Case 3 we get (3.24a) and combining Case 1 and Case 2 leads to (3.24b). The bound of the convergence factor as shown in (3.25) can be deduced from the above analysis straightforwardly. □

Remark 3.3. The method proposed in [22] is geometrical since it depends on the selected box which contains the curve Γ. Clearly, compared to the geometrical method, our method is algebraic and it depends on the selected $\hat{\rho}$ which is an upper

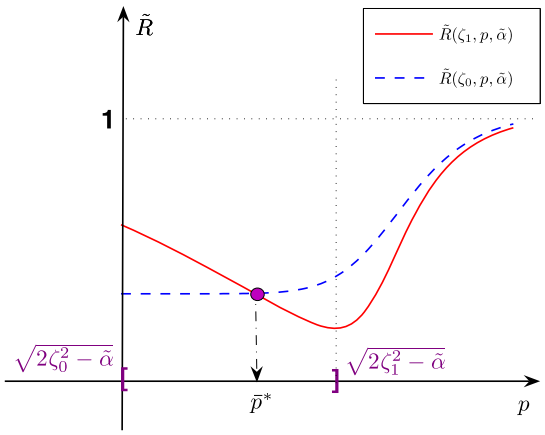

Fig. 3.6. Sketch map of $\tilde{R}(\zeta_0, p, \tilde{\alpha})$ and $\tilde{R}(\zeta_1, p, \tilde{\alpha})$ for $\zeta_0^2 - \zeta_0\zeta_1 - \tilde{\alpha} \leqslant 0$ and $\zeta_1^2 - \zeta_0\zeta_1 - \tilde{\alpha} \geqslant 0$.

of the convergence factor ρ. In Section 4 and Section 5, we will show numerically that the new method can result in a more efficient quasi-optimized parameter.

4. Some comparison results

In this section, we consider the degenerated situation $-\partial_t u - \partial_{xx} u + a_2 u(x, t-\tau) = 0$, i.e., the heat equation with time delay. In [22], by using the geometrical method, i.e., the *box* technique introduced in Section 3.1, Vandewalle and Gander presented the following results for the case $L = 0$.

Theorem 4.1. *(See [22, Theorem 6].) Let $L = 0$ and $b = \Re(\sqrt{i(\omega_{\max} + \frac{2\pi}{\tau}) + a_2 e^{-i\omega_{\max}\tau}})$. Assume $0 < a_2\tau \leqslant 1$, then the solution of the min–max problem over the bounding box is given by*

$$p^* = \begin{cases} \sqrt{2\cos(a_2\tau)b - a_2}, & \text{if } b \geqslant a_2\cos(a_2\tau) + \frac{1}{\cos(a_2\tau)}, \\ \sqrt{2a_2^2\cos^2(a_2\tau) + a_2}, & \text{if } b < a_2\cos(a_2\tau) + \frac{1}{\cos(a_2\tau)}. \end{cases} \tag{4.1}$$

By using the parameter p^*, the convergence factor of the SWR algorithm can be bounded as

$$\rho(p^*, 0) \leqslant \frac{(p^* - a_2\cos(a_2\tau))^2 + a_2^2\cos^2(a_2\tau) + a_2}{(p^* + a_2\cos(a_2\tau))^2 + a_2^2\cos^2(a_2\tau) + a_2}. \tag{4.2}$$

We note that Theorem 4.1 requires $0 < a_2\tau \leqslant 1$ and we do not know whether the parameter p^* given by (4.1) is still efficient or not when $a_2\tau > 1$. But, from the following theorem which is also given in [22], we know that the SWR algorithm (2.2)–(2.3) with Robin transmission conditions (2.4) converges if $0 < a_2\tau \leqslant \frac{\pi}{2}$.

Theorem 4.2. *(See [22, Theorem 5].) Assume a_2 and τ satisfy $0 < a_2\tau \leqslant \frac{\pi}{2}$. Then, the SWR algorithm* (2.2)–(2.3) *with the Robin transmission conditions* (2.4) *converges, whenever $L \geqslant 0$.*

Theorem 4.2 predicts the convergence of the Robin type SWR algorithm (2.2)–(2.4) for both the cases $L > 0$ and $L = 0$, if $a_2\tau \in (0, \frac{\pi}{2}]$. Therefore, it is nature to compare the effectiveness of the two quasi-optimized parameters given by Theorem 3.1 and Theorem 4.1 for $a_2\tau \in (0, \frac{\pi}{2}]$. Due to the complexity of the convergence factor ρ, it is difficult to compare the two methods theoretically and we have to rely on numerical calculations only. Since $L = 0$, it is clear that both methods depend on the quantities a_2 and τ only. We therefore define the *convergence region* of the two methods on "a_2–τ" plane as

$$\mathcal{D} = \left\{ (a_2, \tau) \,\middle|\, a_2 > 0,\ \tau > 0 \text{ such that } \rho(p^*, 0) = \max_{z\in\Gamma} \left| \frac{(z - p^*)^2}{(z + p^*)^2} \right| < 1 \right\}, \tag{4.3}$$

where Γ is the curve along which one needs to solve the min–max problem to find the optimal parameter in the Robin transmission conditions and p^* is the quasi-optimized parameters derived by using the algebraic method (i.e., Theorem 3.1) or the geometrical method (i.e., Theorem 4.1). In what follows, we denote these two quasi-optimized parameters by p^*_{new} and p^*_{old}, respectively.

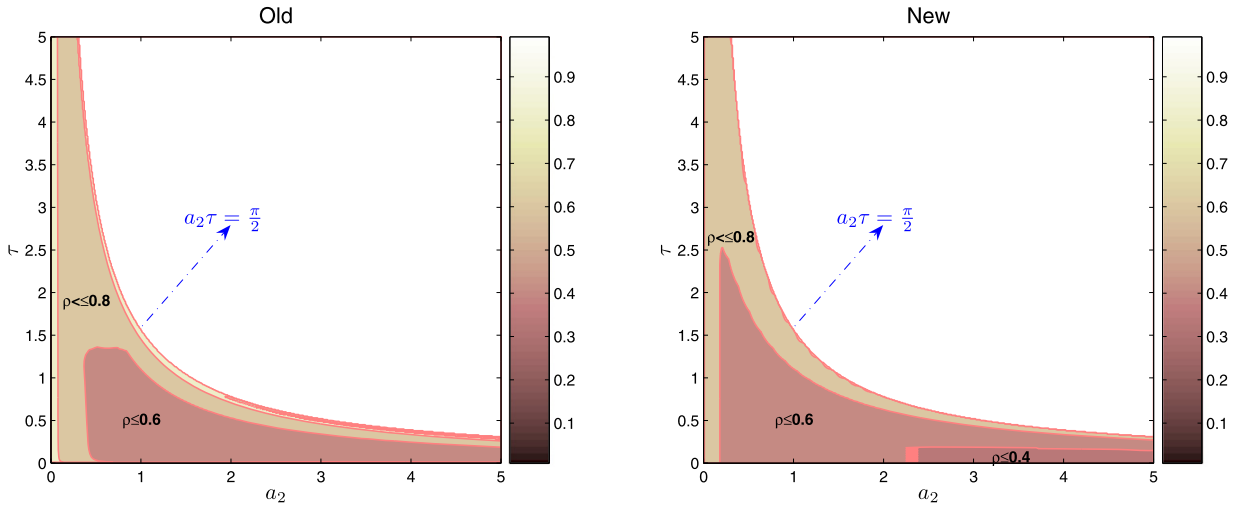

Fig. 4.1. Contour plots of the geometrical method (left) and the algebraic method (right).

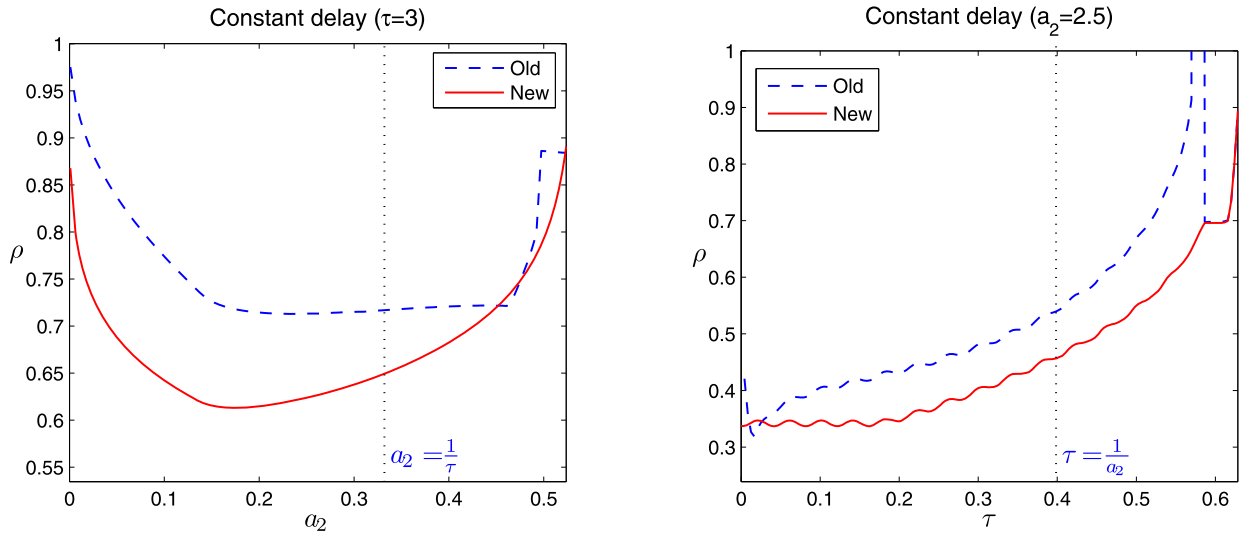

Fig. 4.2. Convergence factors $\rho(p^*_{\text{new}}, 0)$ (solid line) and $\rho(p^*_{\text{old}}, 0)$ (dash line). Left: $\tau = 3$ and a_2 varies from 0 to $\frac{\pi}{2\tau}$; Right: $a_2 = 2.5$ and τ varies from 0 to $\frac{\pi}{2a_2}$.

In Fig. 4.1, we show the contour plots of the two methods for the heat equation with a constant delay, in which we see clearly that for a given quantity $r \in (0, 1)$ such that $\max_{z\in\Gamma} |\frac{(z-p^*)^2}{(z+p^*)^2}| \leqslant r$, the algebraic method allows larger region of (a_2, τ). Moreover, we find numerically that the both methods are valid in a region with boundary curve $a_2\tau = \frac{\pi}{2}$.

We next show that for a given pair of (a_2, τ), the algebraic method also results in a sharper convergence speed of the SWR algorithm. To illustrate this intuitively, for $\tau = 3$ we plot ρ with respect to different a_2 in the left panel of Fig. 4.2. Similarly, in the right panel we plot ρ with respect to different τ when $a_2 = 2.5$ is fixed. From these two panels, we see clearly that the algebraic method is more feasible and results in more efficient parameter.

5. Numerical results

We perform in this section several numerical experiments to measure the effectiveness of the derived quasi-optimized parameter for the numerical implementation of the SWR algorithms. We use the PDE model problem (2.1) with $x \in (0, 4)$ (i.e., $\Omega = (0, 4)$) and $t \in (0, 10)$. We impose homogeneous boundary conditions, $u(0, t) = 0$ and $u(4, t) = 0$, and use various source function $f(x, t)$ and initial condition $u_0(x, t)$ for $(x, t) \in \Omega \times [-\tau, 0]$. We first use a decomposition of the domain Ω into the two subdomains $\Omega_1 = (0, L_2)$ and $\Omega_2 = (L_1, 4)$ with $L_1 \leqslant L_2$, and hence the overlap size $L = L_2 - L_1$.

We show results of numerical experiments for only the algorithm with overlap since with overlap we can compare the results to the classical Schwarz waveform relaxation algorithms with Dirichlet transmission conditions, which does

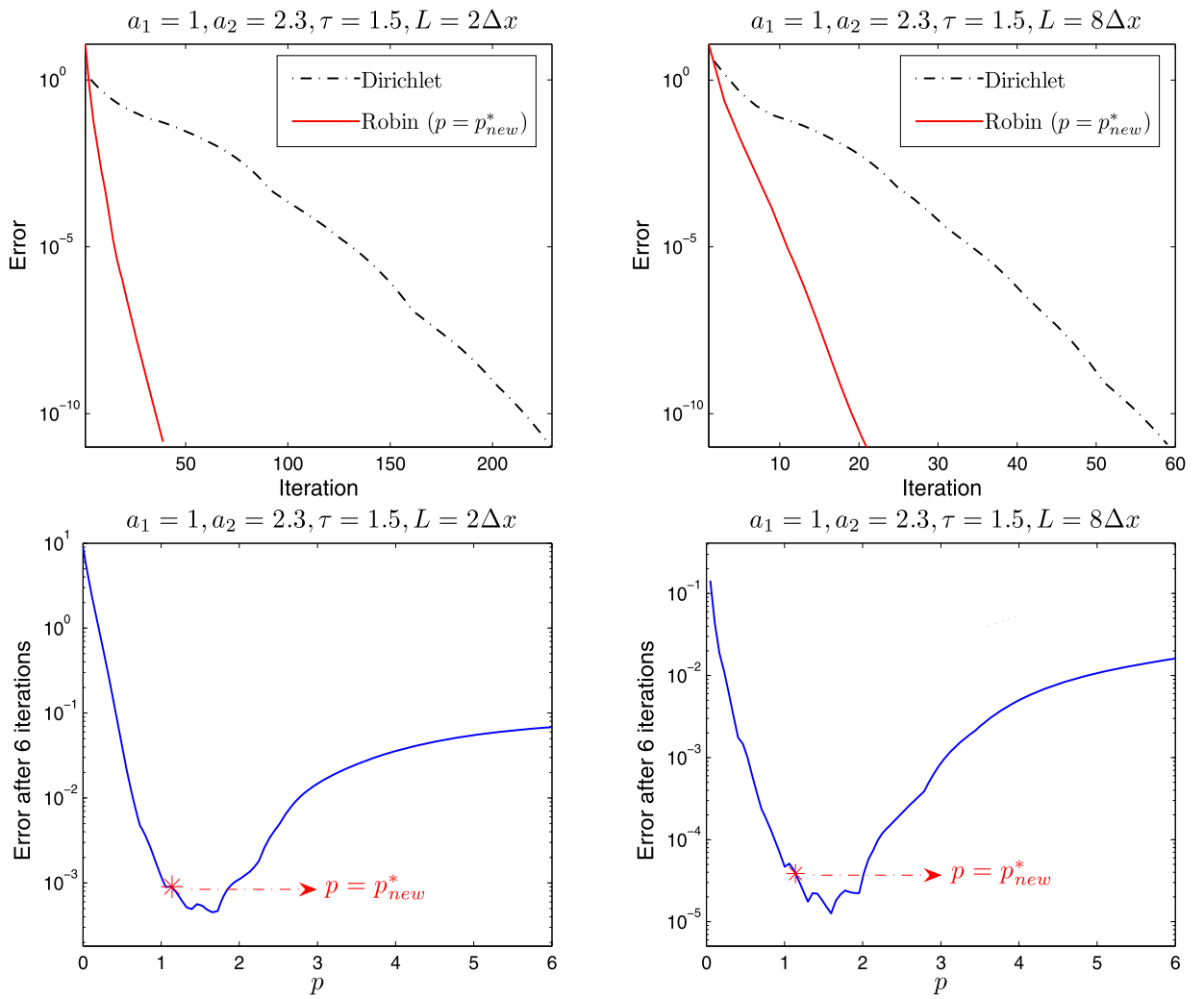

Fig. 5.1. Top: convergence rate of the classical SWR algorithms (dash–dot line) and the Robin type SWR algorithms with parameter $p = p^*_{\text{new}}$ (solid line). Bottom: the errors obtained by running the SWR algorithms with Robin transmission conditions after 6 iterations and various choices of the free parameters p, and indicated by a star the choice $p = p^*_{\text{new}}$.

not converge without overlap. We remark that even though the quasi-optimized parameter p^* is analyzed at the special level $L = 0$, we can use it for the case $L > 0$. Of course, such p^* may be far away from the solution of $\min_{p>0} \rho(p, L) = \min_{p>0} \max_{z\in\Gamma} |\frac{(z-p)^2}{(z+p)^2} e^{-2\frac{z}{v}L}|$. In fact, we will see later that the quasi-optimized parameters p^* given by Theorems 3.1 and 4.1 result in significant acceleration compared to the classical SWR algorithms.

We discretize the fully continuous SWR algorithm (2.2)–(2.3) using the central finite difference discretization in space with mesh parameter $\Delta x = 0.05$ and a backward Euler discretization in time, with time step $\Delta t = 0.02$.

Example 5.1 *(The case $a_1 \neq 0$).* We choose the coefficients $a_1 = 1$, $a_2 = 2.3$ and $\tau = 1.5$ and by using Theorem 3.1, we know that the quasi-optimized parameter $p^*_{\text{new}} = 1.14017563430500$. In this first set of experiments, the initial condition and the source function are chosen as:

$$u_0(x, t) = t \sin(\pi x), \qquad f(x, t) = \cos\left(xe^t\right). \tag{5.1}$$

In Fig. 5.1 on the top, we show the convergence rate of the two kinds of SWR algorithms for $L = 2\Delta x$ (top left) and $L = 8\Delta x$ (top right). We see clearly in these two panels that, compared to the classical SWR algorithms the Robin type SWR algorithms with the quasi-optimized parameter p^*_{new} possesses drastically faster convergence speed. We next verify to what degree the choice for the parameter $p = p^*_{\text{new}}$ derived using the algebraic method corresponds to the best choice one can make in the fully discretized situation. In Fig. 5.1 on the bottom we show the errors obtained after running the SWR algorithms with Robin transmission conditions for 6 iterations using various values for the free parameter p in the

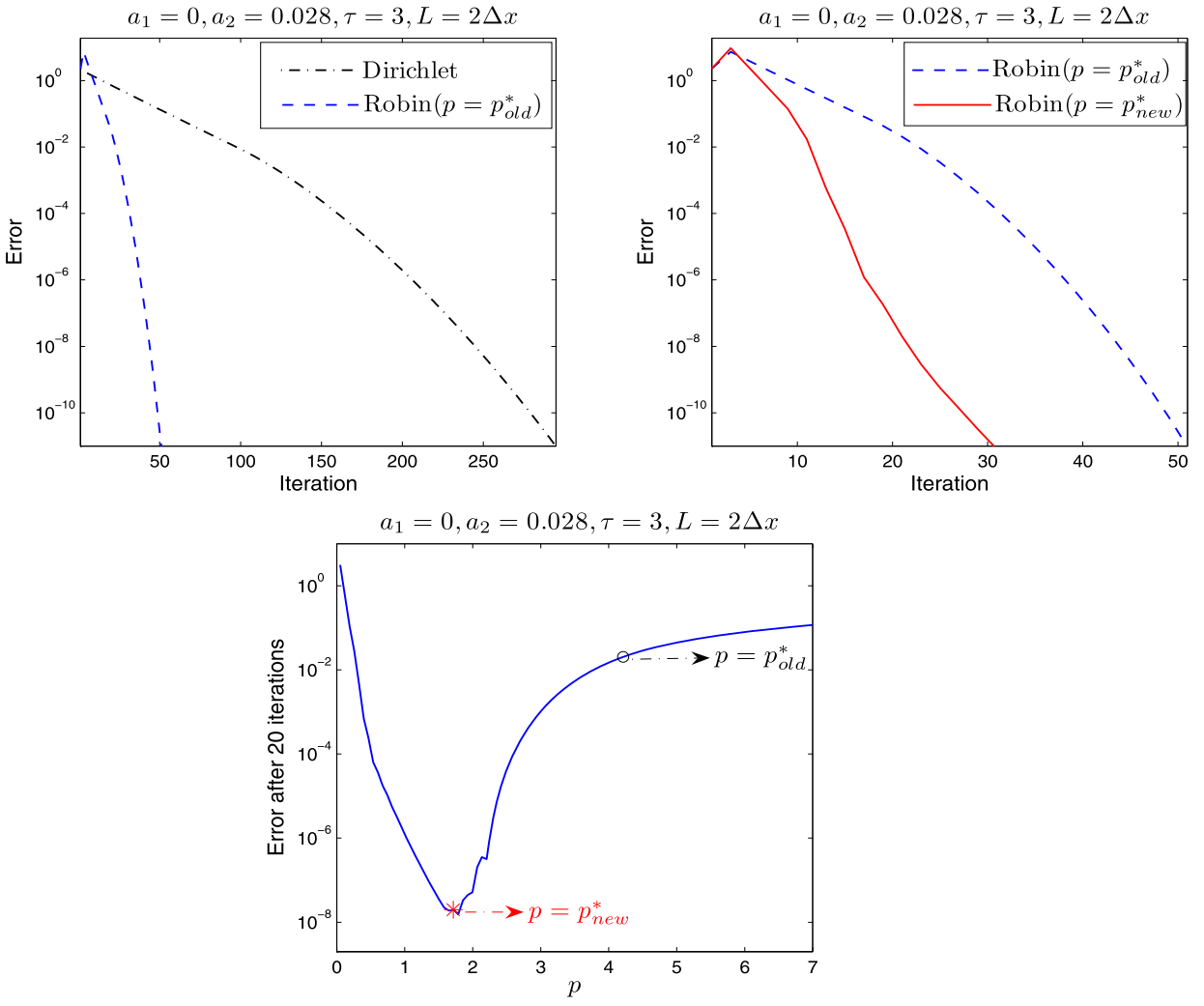

Fig. 5.2. Left: convergence rate of the classical SWR algorithms (dash–dot line) and the Robin type SWR algorithms with parameter $p = p^*_{\text{old}}$ (dash line). Right: convergence rate of the Robin type SWR algorithms with parameters $p = p^*_{\text{new}}$ (solid line) and $p = p^*_{\text{old}}$ (dash line). Bottom: the errors obtained by running the algorithms with Robin transmission conditions after 20 iterations and various choices of the free parameters p, and indicated by a star and a circle the choices $p = p^*_{\text{new}}$ and $p = p^*_{\text{old}}$, respectively.

transmission conditions; the left and right panels correspond to the result for the case of $L = 2\Delta x$ and $L = 8\Delta x$, respectively. In each panel, the choice $p = p^*_{\text{new}}$ is indicated by a star. One can find in these two panels that the quasi-optimized parameter $p = p^*_{\text{new}}$ analyzed in the special level $L = 0$ predicts the best one well.

Example 5.2 *(The case $a_1 = 0$).* We now consider the case $a_1 = 0$ in (2.1), i.e., the heat equations with a constant delay. We compare the performance of the two quasi-optimized parameters $p = p^*_{\text{new}}$ and $p = p^*_{\text{old}}$, which are predicted by Theorems 3.1 and 4.1, respectively. We choose the initial condition and the source function in (2.1) as:

$$u_0(x,t) = 1 + \cos\left(e^{t\sin(\pi x)}\pi\right), \qquad f(x,t) = (x-1)(x-3)\sin\left(xt^2\right). \tag{5.2}$$

Let $a_2 = 0.028$, $\tau = 3$ and then we get the two quasi-optimized parameters: p^*_{new}=1.71410236659459 and $p^*_{\text{old}} =$ 4.21342663346202. Here we consider $L = 2\Delta x$ and in Fig. 5.2 on the left we show the convergence rate of the classical SWR algorithms (dash–dot line) and the Robin type SWR algorithms (dash line) with $p = p^*_{\text{old}}$, in which one can see the significant acceleration effect of the Robin type transmission conditions. To illustrate the difference between p^*_{old} and p^*_{new} intuitively, we show the convergence rate of the Robin type SWR algorithms with $p = p^*_{\text{old}}$ (dash line) and $p = p^*_{\text{new}}$ (solid line) in a single panel—the right panel of Fig. 5.2, in which one can see how much faster the algorithm with $p = p^*_{\text{new}}$ converges compared to the one with $p = p^*_{\text{old}}$.

Next, we verify to what degree the choices for the parameter $p = p^*_{\text{new}}$ and $p = p^*_{\text{old}}$ derived using the algebraic method and the geometrical method correspond to the best choice one can make in the fully discretized situation with $L > 0$. In

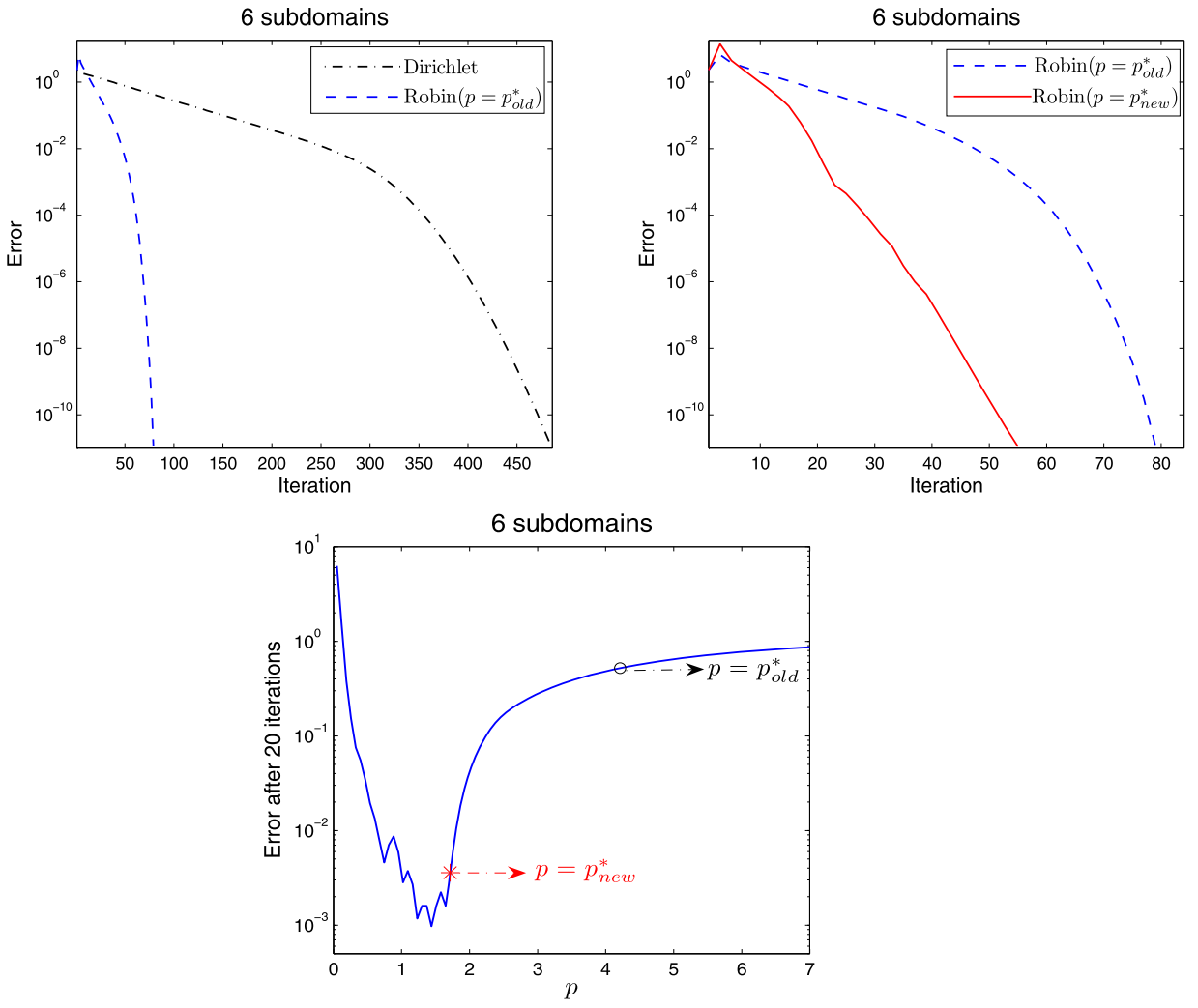

Fig. 5.3. Convergence behavior of the SWR algorithms in many subdomain case. Left: convergence rate of the classical SWR algorithms (dash–dot line) and the Robin type algorithms with parameter $p = p^*_{\text{old}}$ (dash line). Right: convergence rate of the Robin type SWR algorithms with parameters $p = p^*_{\text{new}}$ (solid line) and $p = p^*_{\text{old}}$ (dash line). Bottom: the errors obtained by running the algorithms with Robin transmission conditions after 20 iterations and various choices of the free parameters p. The choices $p = p^*_{\text{new}}$ and $p = p^*_{\text{old}}$ are indicated by a star and a circle, respectively.

Fig. 5.2 on the bottom, we show the errors obtained after running the SWR algorithms with Robin transmission conditions for 20 iterations using various values for the free parameter p in the transmission conditions. The choices $p = p^*_{\text{new}}$ and $p = p^*_{\text{old}}$ are indicated by a star and a circle, respectively. One can find in this panel that the quasi-optimized parameter $p = p^*_{\text{new}}$ analyzed in the special level $L = 0$ predicts the best choice very well and particularly much better than $p = p^*_{\text{old}}$.

Example 5.3 *(The case of many subdomains).* To finish this section, we now show experiments which indicate that the results we obtained for two subdomains are also relevant for many subdomains. Using the same model problem and the same parameters for the SWR algorithms as in Example 5.2, we now decompose the domain into 6 subdomains and the results are shown in Fig. 5.3. One can see on the left how important the transmission conditions are in the many subdomain case. Again, to illustrate the difference between p^*_{old} and p^*_{new} intuitively in many subdomain situation, we show the convergence rate of the Robin type SWR algorithms with $p = p^*_{\text{old}}$ (dash line) and $p = p^*_{\text{new}}$ (solid line) in a single panel|the right panel of Fig. 5.3, in which one can see clearly that $p = p^*_{\text{new}}$ is also a much better choice than $p = p^*_{\text{old}}$. In particular, the iteration number for the algorithm with $p = p^*_{\text{new}}$ and $p = p^*_{\text{old}}$ is 55 and 80, respectively. Like what we have done in Example 5.2, we show in the bottom panel the errors obtained by running the algorithm with Robin transmission conditions after 20 iterations and various choices of the free parameters p, and indicated by a star and a circle the choices $p = p^*_{\text{new}}$ and $p = p^*_{\text{old}}$, respectively. In this panel, we can see clearly that the new choice $p = p^*_{\text{new}}$ still outperforms the old one, and compared to the two subdomain case, both $p = p^*_{\text{new}}$ and $p = p^*_{\text{old}}$ are much more far away from the best choice.

Remark 5.1. We have theoretically shown in Remark 3.1 that when the overlap size $L = 0$, the SWR algorithms with Robin transmission conditions are convergent, but the ones with Dirichlet transmission conditions (i.e., the classical SWR algorithms) are not. Here, we further compare the two types of transmission conditions for the case $L > 0$ by several numerical results. From the results, we can see that the SWR algorithms with Robin transmission conditions are convergent greatly faster than the ones with Dirichlet transmission conditions, provided the parameter involved in the Robin transmission conditions is chosen properly.

6. Conclusion and discussion

SWR algorithms have been investigated deeply and widely for regular PDEs, while there is little experience of this kind of algorithms for PDEs with delay. In this paper, we focus on investigating the convergence behavior of the algorithms with Robin type transmission conditions, in which a free parameter p is involved. We use the reaction diffusion equations with a constant delay as the underlying model problem and try to determine the best parameter in the transmission conditions. We propose the algebraic method to obtain a quasi-optimized parameter $p = p^*_{\text{new}}$. The key point for this method lies in constructing a proper upper bound of the convergence factor. Such upper bound contains the free parameter p and the min–max problem concerned with this bound can be solved in closed formulas. For the case $L = 0$, it is shown that the SWR algorithms with Robin transmission conditions can be convergent with satisfactory convergence rate by using the quasi-optimized parameter $p = p^*_{\text{new}}$, while in theory the SWR algorithms with transmission conditions of Dirichlet type are not convergent (see Remark 3.1). Moreover, for the case $L > 0$, we have shown numerically that the Robin transmission conditions with parameter p^*_{new} can remarkably outperform the Dirichlet transmission conditions in the sense of convergence speed.

When the situation is reduced into the heat equations with a constant delay, it is shown that the algebraic method outperforms the geometrical method introduced in [22]. In particular, the algebraic method has two significant merits:

(a) it allows larger region of (a_2, τ). In particular, the restriction $a_2\tau \in (0, 1]$ required in [22] can be removed and for $a_2\tau \in (0, \frac{\pi}{2}]$ the algebraic method can still result in suitable quasi-optimized parameter;
(b) for given a_2 and τ which satisfy $0 < a_2\tau \leqslant \frac{\pi}{2}$, the algebraic method results in more efficient parameter for the Robin transmission conditions.

There are still some important problems that need to be answered. Firstly, we only considered the case $L = 0$ which is very special in the field of SWR algorithms. For the general case $L > 0$, the min–max problem becomes more complex and therefore it is difficult to be analyzed. In our forthcoming paper, we will generalize the algebraic method proposed in this paper to the case $L > 0$.

The second problem is the generalization of this method to the 2D or 3D case. This generalization is far from obvious. A first step in this direction can be quite easily performed, which consists in deriving the general form of the errors in the Fourier space. In a similar way to what was done in the 1D case, these errors are expressed in terms of λ_+ and λ_-. However, the expressions of λ_+ and λ_- are quite complicated, which makes it very difficult to derive relevant results in such a general case.

Acknowledgments

The authors would like to thank the anonymous referees, the editor Prof. Chen Goong for their constructive suggestions and comments. This work was supported by the NSF of Sichuan University of Science and Engineering (2010X JKRL005) and the NSF of China (10971077).

References

[1] D. Bennequin, M.J. Gander, L. Halpern, A homographic best approximation problem with application to optimized Schwarz waveform relaxation, Math. Comp. 78 (2009) 185–223.
[2] D.S. Daoud, M.J. Gander, Overlapping Schwarz waveform relaxation for advection diffusion equations, Bol. Soc. Esp. Mat. Apl. SeMA 46 (2009) 75–90.
[3] D.S. Daoud, I. Caltinoglu, Overlapping Schwarz waveform relaxation method for the solution of the reaction–diffusion equation, J. Math. Anal. Appl. 333 (2007) 1153–1164.
[4] D.S. Daoud, Overlapping Schwarz waveform relaxation method for the solution of the forward–backward heat equation, J. Comput. Appl. Math. 208 (2007) 380–390.
[5] V. Dolean, M.J. Gander, L. Gerardo-Giorda, Optimized Schwarz methods for Maxwell's equations, SIAM J. Sci. Comput. 31 (2009) 2193–2213.
[6] M.J. Gander, H. Zhao, Overlapping Schwarz waveform relaxation for the heat equation in n-dimensions, BIT Numer. Math. 42 (2002) 779–795.
[7] M.J. Gander, A.M. Stuart, Space–time continuous analysis of waveform relaxation for the heat equation, SIAM J. Sci. Comput. 19 (1998) 2014–2031.
[8] M.J. Gander, L. Halpern, S. Labbe, K. Santugini-Repiquet, An optimized Schwarz waveform relaxation algorithm for micro-magnetics, in: Proceedings of the 17th International Conference on Domain Decomposition Methods, 2007.
[9] M.J. Gander, C. Rohde, Overlapping Schwarz waveform relaxation for convection-dominated nonlinear conservation laws, SIAM J. Sci. Comput. 27 (2005) 415–439.
[10] E. Giladi, H.B. Keller, Space–time domain decomposition for parabolic problems, Numer. Math. 93 (2002) 279–313.
[11] M.J. Gander, H. Zhao, Overlapping Schwarz waveform relaxation for parabolic problems in higher dimension, Proc. Algoritmy 97 (1997) 42–51.
[12] M.J. Gander, Overlapping Schwarz for parabolic problems, in: Proceedings of the 9th International Conference on Domain Decomposition Methods, Domain Decomposition Press, 1997.

[13] M.J. Gander, A waveform relaxation algorithm with overlapping splitting for reaction diffusion equations, Numer. Linear Algebra Appl. 6 (1998) 125–145.
[14] M.J. Gander, L. Halpern, Optimized Schwarz waveform relaxation for advection reaction diffusion problems, SIAM J. Numer. Anal. 45 (2007) 666–697.
[15] E. Lelarasmee, A.E. Ruehli, A.L. Sangiovanni-Vincentelli, The waveform relaxation methods for time-domain analysis of large scale integrated circuits, IEEE Trans. Comput.-Aided Des. 1 (1982) 131–145.
[16] J.L. Lions, E. Magenes, Problèmes aux limites non homogènes et applications, Trav. Recherches Math., vols. 17–18, Dunod, Paris, 1968.
[17] V. Martin, An optimized Schwarz waveform relaxation method for the unsteady convection diffusion equation in two dimensions, Appl. Numer. Math. 52 (2005) 401–428.
[18] H. MacMullen, E. O'Riordan, G.I. Shishkin, The convergence of classical Schwarz methods applied to convection–diffusion problems with regular boundary layers, Appl. Numer. Math. 43 (2002) 297–313.
[19] V. Martin, Schwarz waveform relaxation algorithms for the linear viscous equatorial shallow water equations, SIAM J. Sci. Comput. 31 (2009) 3595–3625.
[20] A. Qaddouri, L. Laayouni, S. Loisel, J. Cote, M.J. Gander, Optimized Schwarz methods with an overset grid for the shallow-water equations: preliminary results, Appl. Numer. Math. 58 (2008) 459–471.
[21] S. Vandewalle, Parallel Multigrid Waveform Relaxation for Parabolic Problems, B.G. Teubner, Stuttgart, 1993.
[22] M.J. Gander, S. Vandewalle, Optimized Overlapping Schwarz Methods for Parabolic PDEs with Time-Delay, Lecture Notes in Comput. Sci., vol. 40, 2005, pp. 291–298.
[23] J. Wu, Theory and Applications of Partial Functional Differential Equations, Springer-Verlag, New York, 1996.
[24] S.L. Wu, C.M. Huang, Ting-Zhu Huang, Convergence analysis of overlapping Schwarz waveform relaxation algorithm for reaction diffusion equations with time-delay, IMA J. Numer. Anal., in press.
[25] B. Zubik-Kowal, S. Vandewalle, Waveform relaxation for functional differential equations, SIAM J. Sci. Comput. 21 (1999) 207–226.